Dielectric properties of interfacial water and distribution of ions at the air/water interface

Chiang, K.-Y.

Publication date
2023

Chapter 6. Vibrational Couplings and Energy Transfer Pathways of Water's Bending Mode

The work presented in this chapter has been published and is reprinted with permission from:
C.-C. Yu*, **K.-Y. Chiang***, et al. "Vibrational couplings and energy transfer pathways of water's bending mode" *Nature Commun.*, 11, 5977 (2020).

Author contributions: Y.N. and J.H. conceived the research idea; C.-C.Y. and K.-Y.C. conducted the IR and pump-probe IR experiments; and M.O. conducted the Raman and hyper-Raman experiments; C.-C.Y., K.-Y.C., and J.H. analyzed the experimental data; Y.N. and T.O. carried out the simulations and analyzed the simulation data; C.- C.Y., K.-Y.C., M.O., T.S., T.O., X.Y., V.K., H.H., M.B., J.H., and Y.N. discussed and interpreted the results; C.-C.Y., K.-Y.C., M.B., J.H., and Y.N. wrote the manuscript.

6.1 Introduction

Liquid water is important as a solvent, a solute, a reactant, and a catalyst, in the environment and many technological applications, but also in biology, driving protein folding and structuring nucleic acids. Many of the unique properties of water originate from the hydrogen bond (H-bond) network of water, which results from the strong intermolecular interactions between water molecules. For instance, the water H-bond network allows for rapid delocalization and dissipation of excess energy following chemical reactions, thereby making reactions irreversible. Insights into the flow of excess vibrational energy in water have therefore been deemed essential for understanding this anomalous liquid.[7,178]

The vibrational modes of liquid H_2O consist of the O-H stretch mode, the H-O-H bending mode, the three librational modes, and collective modes below 100 cm^{-1}. The 3000-4000 cm^{-1} O-H stretch mode has been most intensely studied, owing to its strong response.[179] Both experimental and simulation studies of the O-H stretch mode have demonstrated different parallel pathways of vibrational energy transfer: between the two OH groups within one water molecule, and between different water molecules.[7,23,32,180,181] Within one molecule, coupling can occur between the symmetric and antisymmetric O-H stretch modes,[26] and the stretch modes are coupled to the bending mode and its overtone.[21,22,28,29,34,54,182–184] The O-H stretch vibration in liquid water is quasi-instantaneously delocalized across several water molecules, and is strongly coupled to the bending mode. As such, the bend vibration in liquid water is an important intermediate in the vibrational relaxation of the excited O-H stretch vibration to the hot ground state.[185–188]

Remarkably, although the stretching mode has been intensely investigated, information on energy transfer pathways from the H-O-H bending mode is lacking. With approximately half the energy of the stretch mode, the bending mode likely provides an efficient pathway for energy delocalization and dissipation. The few experimental and theoretical studies of the bending mode have revealed that the delocalized character of H-O-H bending mode affects the vibrational dynamics,[33,34,36] but the impact

of the delocalization on the dynamics is still under debate. For example, the impact of the intermolecular bending-bending vibrational coupling (Figure 6.1a)[33,34,36] as well as the vibrational coupling of the bending and librational modes (Figures 6.1b and 6.1c)[21,35,36,54,183] have been separately investigated, while there is no systematic study for these mechanisms. Furthermore, the impact of the bending mode-librational mode mixing (Figure 6.1d) on the dynamics has not been identified, though recent studies imply the importance of the mode mixing beyond the normal mode description.[22,34] This missing understanding of water's bending mode vibrational dynamics precludes a unified view of vibrational energy exchange and relaxation of water vibrations.

In this chapter, we explore the energy dynamics of the bend vibration by directly comparing vibrational energy relaxation dynamics and randomization of the transition dipole orientation for the bending mode in H_2O-D_2O mixtures. Lowering the H_2O concentration allows suppressing the effect of intermolecular coupling, while keeping the local environment unchanged. Our results show that the intermolecular coupling of the bend vibration is relatively weak in contrast to the stretch vibration. In line with earlier reports,[7,179,189] we find intermolecular vibrational energy relaxation to occur on a sub-picosecond timescale. Yet, our results suggest that intermolecular bend-to-bend energy transfer is much slower (~1 ps) than the intermolecular stretch-to-stretch transfer (~0.1 ps). Randomization of the orientations for the H-O-H bending mode transition dipole moment occurs much faster, which is attributed to rotational contributions (e.g., librational mode) to the bending mode band.

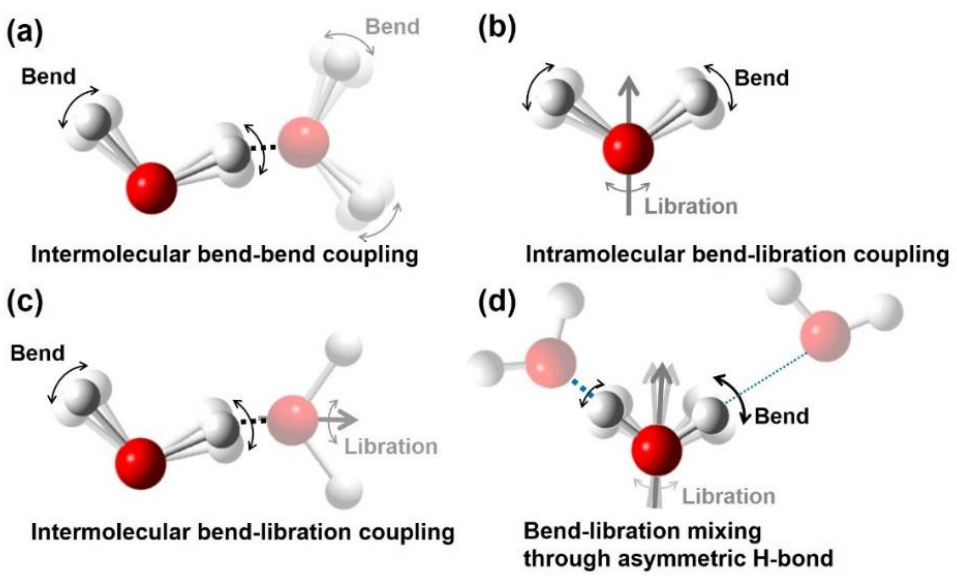

Figure 6.1. Types of the vibrational couplings of the H-O-H bending mode. (a) Intermolecular bend-bend coupling of different water molecules. (b) Intramolecular bend-libration coupling within a single water molecule. (c) Intermolecular bend-libration coupling of different water molecules. (d) Bend-libration mixing induced by the asymmetric hydrogen-bond (H-bond) strengths.

6.2 Materials and Methods

6.2.1 Pump-Probe IR Experiments

The details were described in Section 2.2.

6.2.2 Simulation Protocol

AIMD simulation and analysis were performed by Tatsuhiko Ohto and Yuki Nagata. We used the *ab initio* molecular dynamics (AIMD) trajectories at the revPBE0-D3(0) level of theory[87,190,191] as well as the classical force field molecular dynamics trajectories with the POLI2VS model.[74] The AIMD simulations employed the QUICKSTEP method[88] implemented in the CP2K program.[89] The auxiliary density matrix method (ADMM) was used[192] to reduce the computational cost for hybrid-generalized gradient approximation (GGA) calculations. We used the mixed Gaussian and plane wave approach as implemented in the CP2K code. For the Gaussian part, the TZV2P basis set was used. We set the plane wave density cutoff to 800 Ry. The norm-conserving Goedecker-Teter-Hutter pseudopotentials[91,193] were used to describe the core electrons. We used the *NPT* ensemble, where the target temperature was set to 300 K with canonical sampling through a velocity rescaling thermostat[92] and the pressure was set to 1 atm. The simulation cell contained 64 H_2O molecules. The time step was set to 0.5 fs. We prepared 8 independent samples and run the 15 ps AIMD simulation for equilibrating the systems. The equilibrated water density was 0.95 g/cm^3. Sequentially, we obtained 10 ps AIMD trajectories which were used for computing the spectra.

MD simulation and analysis were performed by Yuki Nagata. For the POLI2VS simulations, we carried out the *NPT* simulation at 300 K. The system temperature was controlled by the Nose-Hoover thermostat. The simulation box contained 500 H_2O molecules. The time step was set to 0.4 fs. We obtained 1 ns trajectories, from which we computed the spectra.

The VDOS spectra were calculated for the dipole moment directions via;[194,195]

$$\mathrm{VDOS}(\omega) = \int_0^T \cos(\omega t)\cos^2\left(\frac{\pi t}{2T}\right)\langle \boldsymbol{v}_i(t)\cdot\boldsymbol{v}_i(0)\rangle dt \tag{6.1}$$

$$\boldsymbol{v}_i(t) = \frac{\left(\boldsymbol{v}_{i,\mathrm{H1}}(t) + \boldsymbol{v}_{i,\mathrm{H2}}(t)\right)}{2} - \boldsymbol{v}_{i,\mathrm{O}}(t), \tag{6.2}$$

where $\boldsymbol{v}_{i,x}(t)$ denotes the velocity vector of atom x=O, H_1, H_2 for water molecule i, T is the length of the time correlation function and was set to 1 ps. The VDOS spectra were decomposed based on the center of mass velocity $\boldsymbol{v}_{i,\mathrm{COM}}(t)$, rotational motion velocity $\boldsymbol{v}_{i,\mathrm{ROT}}(t)$, intramolecular bending motion velocity $\boldsymbol{v}_{i,\mathrm{INTRA(bend)}}(t)$, and intramolecular stretch motion velocity $\boldsymbol{v}_{i,\mathrm{INTRA(stretch)}}(t)$.

$$\boldsymbol{v}_{i,\mathrm{COM}}(t) = \frac{\left(m_\mathrm{H}\boldsymbol{v}_{i,\mathrm{H1}}(t) + m_\mathrm{H}\boldsymbol{v}_{i,\mathrm{H2}}(t) + m_\mathrm{O}\boldsymbol{v}_{i,\mathrm{O}}(t)\right)}{(2m_\mathrm{H} + m_\mathrm{O})} \tag{6.3}$$

$$\boldsymbol{v}_{i,\mathrm{INTRA(bend)}}(t) = c_{i,\mathrm{bend}}(t)\left(-0.33\boldsymbol{u}_{i,\mathrm{OH1}}(t) - 0.33\boldsymbol{u}_{i,\mathrm{OH2}}(t)\right) \tag{6.4}$$

$$\boldsymbol{v}_{i,\mathrm{INTRA(stretch)}}(t) = \boldsymbol{v}_{i,\mathrm{INTRA(s-stretch)}}(t) + \boldsymbol{v}_{i,\mathrm{INTRA(as-stretch)}}(t) \tag{6.5}$$

$$\boldsymbol{v}_{i,\mathrm{INTRA(s-stretch)}}(t) = c_{i,\mathrm{s-stretch}}(t)\left(-0.37\boldsymbol{u}_{i,\mathrm{OH1}}(t) - 0.37\boldsymbol{u}_{i,\mathrm{OH2}}(t)\right) \tag{6.6}$$

$$\boldsymbol{v}_{i,\mathrm{INTRA(as-stretch)}}(t) = c_{i,\mathrm{as-stretch}}(t)\left(-0.42\boldsymbol{u}_{i,\mathrm{OH1}}(t) + 0.42\boldsymbol{u}_{i,\mathrm{OH2}}(t)\right) \tag{6.7}$$

$$\boldsymbol{v}_{i,\mathrm{ROT}}(t) = \boldsymbol{v}_{i}(t) - \boldsymbol{v}_{i,\mathrm{COM}}(t) - \boldsymbol{v}_{i,\mathrm{INTRA(bend)}}(t) - \boldsymbol{v}_{i,\mathrm{INTRA(stretch)}}(t), \tag{6.8}$$

where m_{H} and m_{O} denote the mass of H and O atoms, respectively. $\boldsymbol{u}_{i,\mathrm{OH1}}$ and $\boldsymbol{u}_{i,\mathrm{OH2}}$ represent the unit OH1 and OH2 vectors, respectively, of the water molecule *i*. $c_{i,\mathrm{mode}}(t)$, mode=bend, symmetric-stretch (s-stretch), asymmetric-stretch (as-stretch), is given as follows;

$$\begin{aligned} c_{i,\mathrm{mode}}(t) = (&c_{1,\mathrm{mode}}\boldsymbol{v}_{i,\mathrm{O}}(t)\cdot\boldsymbol{u}_{i,\mathrm{OH1}}(t) + c_{2,\mathrm{mode}}\boldsymbol{v}_{i,\mathrm{O}}(t)\cdot\boldsymbol{u}_{i,\mathrm{OH2}}(t) \\ &+c_{3,\mathrm{mode}}\boldsymbol{v}_{i,\mathrm{H1}}(t)\cdot\boldsymbol{u}_{i,\mathrm{OH1}}(t) + c_{4,\mathrm{mode}}\boldsymbol{v}_{i,\mathrm{H1}}(t)\cdot\boldsymbol{u}_{i,\mathrm{OH2}}(t) \\ &+c_{5,\mathrm{mode}}\boldsymbol{v}_{i,\mathrm{H2}}(t)\cdot\boldsymbol{u}_{i,\mathrm{OH1}}(t) + c_{6,\mathrm{mode}}\boldsymbol{v}_{i,\mathrm{H2}}(t)\cdot\boldsymbol{u}_{i,\mathrm{OH2}}(t))/A_{\mathrm{mode}} \end{aligned}$$

$$A_{\mathrm{mode}} = \sqrt{\left(c_{1,\mathrm{mode}}^2 + c_{2,\mathrm{mode}}^2 + c_{3,\mathrm{mode}}^2 + c_{4,\mathrm{mode}}^2 + c_{5,\mathrm{mode}}^2 + c_{6,\mathrm{mode}}^2\right)}, \tag{6.9}$$

where the coefficients of $c_1, c_2, \cdots, c_6$ for a specific vibrational mode were computed based on the normal mode of the water molecule in the gas phase at the revPBE0-D3(0) level of theory using the ORCA program and were summarized in Table 6.1.[196]

Table 6.1. Coefficients for Vibrational Mode Decomposition.

Mode	c_1	c_2	c_3	c_4	c_5	c_6
bend	0.06	0.06	0.19	-0.73	-0.73	0.19
s-stretch	0.04	0.04	-0.72	0.06	0.06	-0.72
as-stretch	0.05	-0.05	-0.73	0.01	-0.01	0.73

6.3 Results and Discussion

6.3.1 Energy Relation from Water Bending Mode to Lower Frequency Mode Determined by Pump-Probe IR Measurement.

To disentangle these vibrational couplings of the H-O-H bending mode, we carried out time-resolved IR measurement by pumping and probing the H-O-H bending mode in neat H_2O and isotopically diluted water. In these experiments, an intense pump laser pulse excites the bending mode from the vibrational ground state to the first vibrationally excited state, and transient spectral modulations are probed as a function of delay time, t. The excitation reduces absorption at the fundamental frequency of the bending mode (ground state bleach) and increases absorption (excited state absorption) at red-shifted frequencies. We measured the transient absorption spectra with the polarization of the probe light both perpendicular ($\Delta\alpha_{\perp}(\omega,t)$) and parallel ($\Delta\alpha_{\parallel}(\omega,t)$) directions to that of the excitation pulse.

First, we discuss the vibrational energy relaxation (intramode energy transfer) of the H-O-H bending mode. In neat H_2O, the vibrational energy transfer from the bending mode to the librational mode occurs within a single water molecule (intramolecularly, Figure 6.1b) and through energy relaxation from the bending mode of one water molecule to the librational mode of an adjacent water molecule (intermolecularly, Figure 6.1c).[21,35,36,54,183] Through isotopic dilution of water, the intermolecular intermode transfer is altered, because the isotopic dilution shifts the librational mode frequency, changing the vibrational coupling between the bending mode and librational mode.

Figure 6.2a shows the isotropic component of the transient absorption response, $\Delta\alpha_{iso}(\omega,t) = \frac{[\Delta\alpha_{\parallel}(\omega,t)+2\Delta\alpha_{\perp}(\omega,t)]}{3}$, which solely represents energy relaxation and is free from rotational contributions, of the H-O-H bending mode for the H_2O:D_2O = 6:4 sample. With increasing delay time, the excited state population relaxes to the ground state, and the dissipated energy gives rise to a temperature increase, which results in persistent spectral modulations at long delay times. To quantify the vibrational dynamics, we used a four-state kinetic model similar to previous studies,[21,54] in which the four states represent, respectively, ground state, bending mode excited state, intermediate state (e.g. including the librational mode excited state), and hot ground state. Figure 6.2b shows integrated (1649 $cm^{-1} < \omega <$ 1662 cm^{-1}) $\Delta\alpha_{iso}$ signals as a function of delay time together with the overall fit and the contributions of each state of the model; the fit manifests that the four-level model well describes the experimental data very well (Figures 6.2a and 6.2b). Figure 6.2d displays the integrated $\Delta\alpha_{\mathrm{iso}}(\omega,t)$ for various concentrations of H_2O-D_2O mixtures. The time traces are similar for all samples. The relaxation time from the excited state bending mode to the intermediate state (τ_1) is ~200 fs (Figure 6.2c), consistent with previous reports.[34,54] Within experimental uncertainty, τ_1 is insensitive to the isotopic composition. The insensitivity of τ_1 to H_2O concentration reveals that the energy relaxation process is unaffected by the isotopic composition of the water molecules surrounding the excited chromophore.

This suggests that intramolecular (Figure 6.1b), but not intermolecular (Figure 6.1c), bend-libration coupling dictates the vibrational energy relaxation of the bending mode.

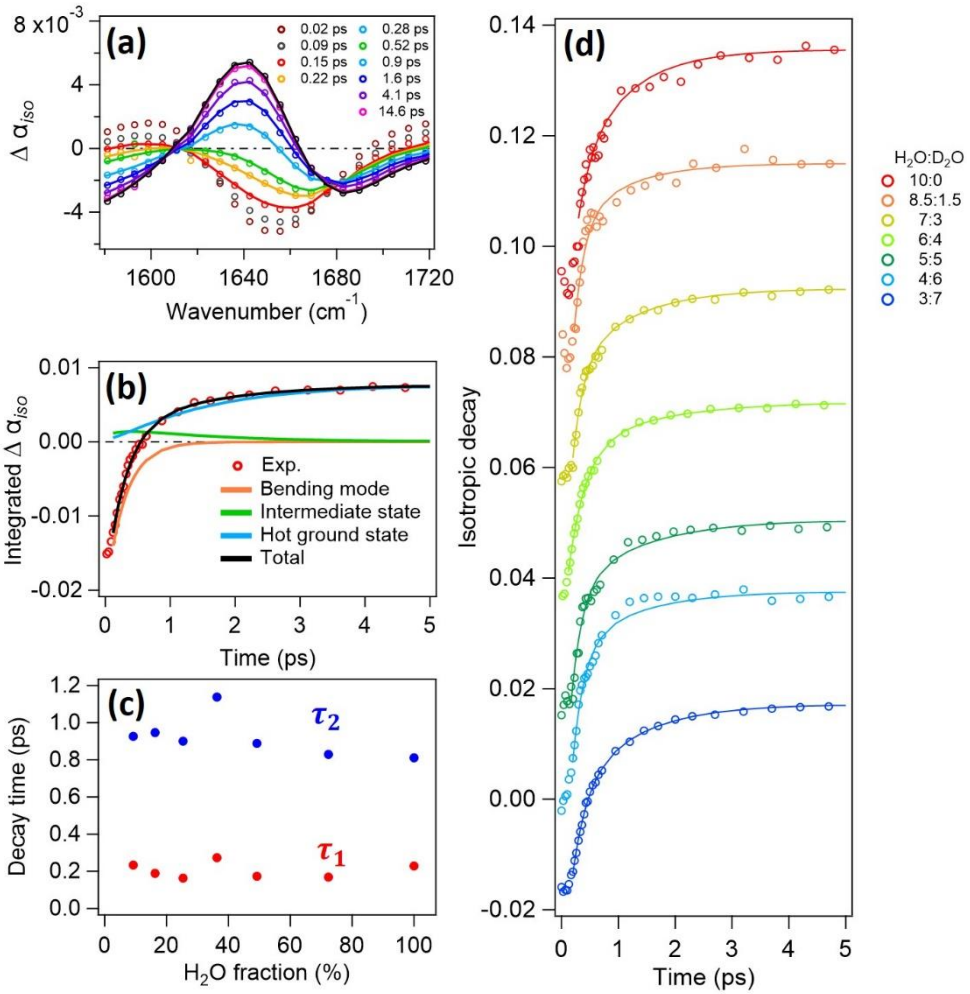

Figure 6.2. The isotropy decay of various isotopic compositions. (a) Transient absorption spectra of water bending mode for H_2O:D_2O = 6:4. The four-state model fit the data start at 0.15 ps. (b) Time evolution of the transient absorption spectra integrated at 1649 $cm^{-1} < \omega < 1662$ cm^{-1}. The orange, green, and blue lines represent the contributions of the excited state, intermediate state, and hot ground state, respectively, to the fit. (c) Isotropic relaxation times as a function of isotopic composition. The lifetime of the excited state to the intermediate state is τ_1 (red symbol) and the lifetime of the intermediate state is τ_2 (blue symbol). (d) Isotropic decay traces for various H_2O-D_2O mixtures. The signals are normalized at t=0. Traces are offset by increments of 0.02. Open circles in panels (a), (b) and (d) represent the experimental data, while the solid lines show fits with the kinetic model.

6.3.2 Intermolecular Bending-Bending Energy Transfer Measured by Polarization-Dependent Pump-Probe IR Measurement.

Figure 6.3a shows the time trace of anisotropy decay for different isotopic compositions. The decay of the excitation anisotropy of the H-O-H bending mode, i.e., the orientational memory of the anisotropic excitation due to polarized light, has provided detailed insight into the coupling of the H-O-H bending chromophores.[32,152] This anisotropy decay is defined as:

$$R(t) = \int_{\omega_1}^{\omega_2} \frac{\Delta\alpha'_{\parallel}(\omega,t) - \Delta\alpha'_{\perp}(\omega,t)}{\Delta\alpha'_{\parallel}(\omega,t) + 2\Delta\alpha'_{\perp}(\omega,t)} d\omega, \tag{6.10}$$

where $\Delta\alpha'_{\perp}(\omega,t)$ and $\Delta\alpha'_{\parallel}(\omega,t)$ represent the transient spectra after the effects of the spectral contribution of the hot ground state (i.e., the spectral signature at long t, in Figure 6.2a)) were subtracted from $\Delta\alpha_{\perp}(\omega,t)$ and $\Delta\alpha_{\parallel}(\omega,t)$, respectively. We set $\omega_1 = 1649$ cm^{-1} and $\omega_2 = 1662$ cm^{-1} in equation (6.10), similar to a previous study.[34]

In contrast to the isotropic transient signals, the excitation anisotropy provides insight into the randomization of the transition dipole orientation of the excited chromophore. Such orientational randomization for neat H_2O can arise from three mechanisms; firstly, the rotational motion of water, and secondly, the loss of the orientational information through exciton hopping to a neighboring water molecule with a differently aligned transition dipole (facilitated by intermolecular bend-to-bend coupling, Figure 6.1a), and thirdly fluctuations caused by bend-libration mixing (Figure 6.1d), which all accelerate the decay of the excitation anisotropy. In isotopically diluted water, the contribution due to intermolecular bend-to-bend energy transfer is suppressed, because of the frequency mismatch of the H-O-H bending mode and H-O-D/D-O-D bending modes. As such, in analogy to the OH stretching band,[32,152] one can quantify the intermolecular bend-to-bend energy transfer from the anisotropy decay of different isotopic compositions.

The time evolution of the anisotropy is displayed in Figure 6.3a. The anisotropy of H_2O molecules in neat H_2O decays with a timescale of ~300 fs. This decay is somewhat slower than that previously reported for neat H_2O,[33,34] which can likely be attributed to the different procedure to subtract the contributions of the hot ground state from the data. The anisotropy decay times, as obtained from fitting exponential decay functions to the data, slows down from 310 ± 20 fs to 440 ± 20 fs upon addition of D_2O. This starkly contrasts with the O-H stretch mode, which shows >10 times faster anisotropy decay in neat H_2O than in isotopically diluted water due to the stretch-stretch modes coupling/energy transfer (see Figure 6.3b).[7,32] The weaker variation of the anisotropy with isotopic composition may be rationalized by the smaller transition dipole moment of the bending mode of water. Assuming that the variation of the anisotropy decay can be fully ascribed to intermolecular bend-to-bend energy transfer, we estimate the contribution of bend-to-bend transfer in neat water from the difference in the decay rates at the two most extreme isotopic compositions of the present study to $((310\text{ fs})^{-1} - (440\text{ fs})^{-1})^{-1}$ = 1.05 ± 0.3 ps. As such, the intermolecular intramode transfer is rather

limited, in stark contrast to the O-H stretch mode exhibiting strong intermolecular intramode vibrational couplings. In turn, the vibrational energy transfer pathway from H_2O bending modes seems to be governed by the energy relaxation to the librational motion. This is summarized in Figure 6.3c.

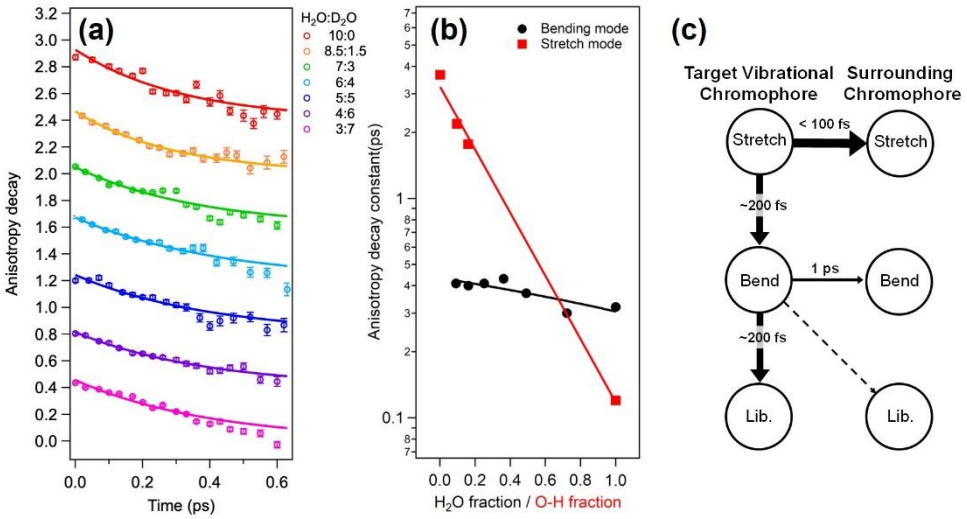

Figure 6.3. The anisotropy decay of various isotopic composition and schematic for the vibrational energy relaxation of water molecules. (a) Anisotropy decay for various H_2O-D_2O mixtures. To obtain the excitation anisotropy, the signals arising from the hot ground state were subtracted from the raw data. Anisotropy decay signals were integrated at 1649 cm-1 < ω < 1662 cm-1. Traces are offset by increments of 0.4. Symbols show experimental data and solid lines show fits using a single exponential decay. (b) Comparison of the anisotropy decay for bending mode and stretch mode as a function of H_2O/O-H fraction. The stretch mode decay times were obtained by fitting an exponential decay to the data reported in Ref. [32]. The lines serve to guide the eye. (c) The schematic representation for the vibrational energy relaxation of H-O-H molecules in neat water. The stretch mode timescales were taken from Refs.[22,31,170,189]. The target vibrational chromophore is the initial excited H-O-H molecule. The surrounding chromophores are the water molecules that surround the excited molecule.

6.3.3 Discussion

The fact that the anisotropy of the bending excitation decays on a 440 fs time scale, which is much faster than the reorientation time of a water molecule (i.e., the H-O-H angular bisector orientational decay of 1.9 ps[197]) strongly suggests that vibrational modes other than the pure bending motion contribute to the observed band at ~1650 cm^{-1}.[34] If the 1650 cm^{-1} band contains vibrational contributions other than a pure bending motion of waters protons, the detected anisotropy decay does not solely arise from the pure rotational motion of the water molecule, rationalizing the different time scales obtained from, e.g., IR pump-probe experiments on isotopically diluted HOD molecules and NMR experiments.[198,199]

To elucidate the exact origin of the vibrational response at 1500-1600 cm^{-1}, we computed the vibrational density of states (VDOS) spectra from the velocity autocorrelation as obtained from AIMD simulations at the revPBE0-D3(0) level of theory as well as from classical force field simulation with the POLI2VS model. We decomposed the vibrational response based on the decomposition of the velocity into the components that arise from the rotational motion (ROT) of an entire water molecule and the intramolecular motion (INTRA). We further decomposed the INTRA motion into the O-H stretching motion that goes along with a variation of the O-H distances and into bending contributions, which mainly involves the variation of the H-H distance. The thus decomposed VDOS spectra are displayed in Figures 6.4a and b.

The simulated VDOS spectra show that the 1650 cm^{-1} feature is not only governed by the intramolecular vibrational motion but also contains contributions from the rotational motion of water molecules. Interestingly and perhaps surprisingly, the pure bending motion, which is not accompanied by a simultaneous rotational motion of water, only accounts for 30 % of the 1650 cm^{-1} VDOS feature. The largest contribution arises from the cross-correlation terms of the bending motion and rotational motion through the mixing of the bending mode and the librational modes (see Figure 6.1d). As such, the simulations confirm the strong coupling of the bending mode to water's librations, giving rise to the 1650 cm^{-1} band. The marked rotational contributions to the 1650 cm^{-1} peak can be rationalized by the notion that – in contrast to water in the gas phase – in liquid water the heterogeneity of hydrogen-bond strengths around a water molecule makes the bending mode potential asymmetric with respect to the bisector (Figure 6.4c).[200,201] The vibrational coordinate of the 1650 cm^{-1} mode contains both rotational motions of the water molecule and a modulation of the H-H distance. In contrast to the band at 1650 cm^{-1}, the band at 3200 - 3600 cm^{-1} can be primarily explained by a proton motion along the O-H axis, that is, the stretching vibration (Figures 6.4a and b).

Together, the rotational contributions to the 1650 cm^{-1} mode make the orientation of its transition dipole differ from the H-O-H angular bisector (Figure 6.4c), and the anisotropy decay of the pump-probe experiments probes the motion of an axis different from the H-O-H angular bisector directions. Since the orientation of the transition dipole moment varies with the hydrogen bond strength of water as is schematically depicted in the bottom panel of Figure 6.4c, the acceleration of the anisotropy decay with respect to the pure H-O-H bisector orientational motion can be linked to the hydrogen bond dynamics. In fact, the acceleration can be estimated to $((440\ fs)^{-1} - (1.9\ ps)^{-1})^{-1} = 570$ fs. The 570 fs time scale agrees with the time constant of the hydrogen bond dynamics of 0.5-1.0 ps, as characterized by the spectral diffusion for the O-H stretch of dilute HOD in D_2O.[195,202,203,204] As such, large bending-libration mode mixing rationalizes the observation that the excitation anisotropy for the 1650 cm^{-1} band (~ 440 fs) of isotopically diluted water as measured in the pump-probe IR measurement decays much faster than the orientation of the bisector as measured using NMR (~ 1.9 ps).[197] The weak mode mixing for the stretch mode is further consistent with the observation that the anisotropy decay

of the O-H stretch mode at ~3400 cm^{-1} for isotopically diluted water (≈ 3-4 ps[32,202,205]) is comparable to the orientational correlation time as detected with NMR (decay ≈ 2 ps[206–209]).

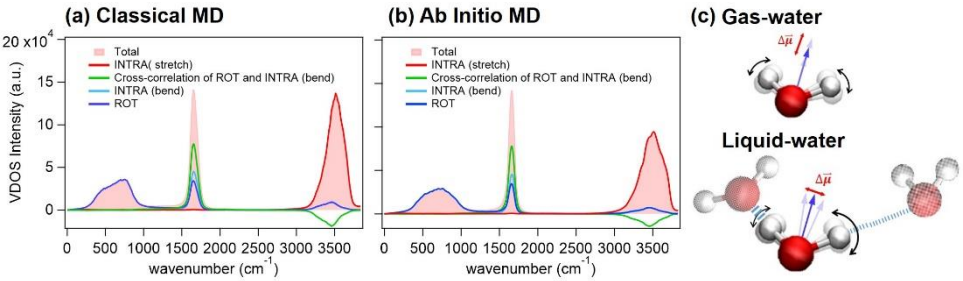

Figure 6.4. Decomposed VDOS spectra of neat H_2O. (a) classical force field MD with the POLI2VS model[74] and (b) AIMD simulation at the revPBE0-D3(0) level of theory. The frequency of the POLI2VS model is scaled with a factor of 0.96 to account for nuclear quantum effects. The frequencies of the bending and stretch modes for the revPBE0-D3(0) model are corrected via the procedure described in Ref. [210]. The red region illustrates the total VDOS spectrum of neat H_2O. The differently colored lines represent the contribution of different motions. (c) Schematics of water molecules in the gas and liquid phase. Strong (weak) hydrogen bonds are represented by thick (thin) broken lines. The blue arrows represent the direction of the dipole moment of the highlighted water molecule, while the red lines represent the direction of the change in the dipole moment (transition dipole moment, $\Delta\vec{\mu}$).

6.4 Conclusion

We quantified the vibrational coupling of the water bending mode, employing time-resolved vibrational spectroscopic techniques. The time-resolved IR measurements reveal that the intermolecular bend-to-bend (intramode) coupling is much weaker than the intermolecular stretch-to-stretch coupling. The intramolecular bend-to-libration energy transfer (≈ 200 fs) takes place much faster than the intermolecular bend-to-bend coupling (≈ 1 ps). As such, the vibrational energy of the bending mode is mainly released not to the bending modes of surrounding water molecules but to the librational mode, in stark contrast to the stretch mode. AIMD simulations confirm strong bend-libration coupling, which can explain the faster decay of the excitation anisotropy of the bending mode (≈ 0.4 ps), much faster than for the stretch mode (≈ 2-4 ps). The experimental and simulation results demonstrate that the librational mode plays a key role in the energy transfer pathway and orientational dynamic of the bending mode band.